

## Supplementary material for LHCb-PAPER-2018-013

This figure shows the invariant mass spectra for  $\Lambda_b^0 \rightarrow \Lambda_c^+ \pi^-$ ,  $\Lambda_b^0 \rightarrow \Lambda_c^+ \mu^- X$  and  $\Xi_b^0 \rightarrow \Xi_c^+ \mu^- X$  candidates for the combined 7, 8 and 13 TeV data sets. Also shown are the combined mass difference distributions for the  $\Xi_b(6227)^-$  candidates in each of the above final states.

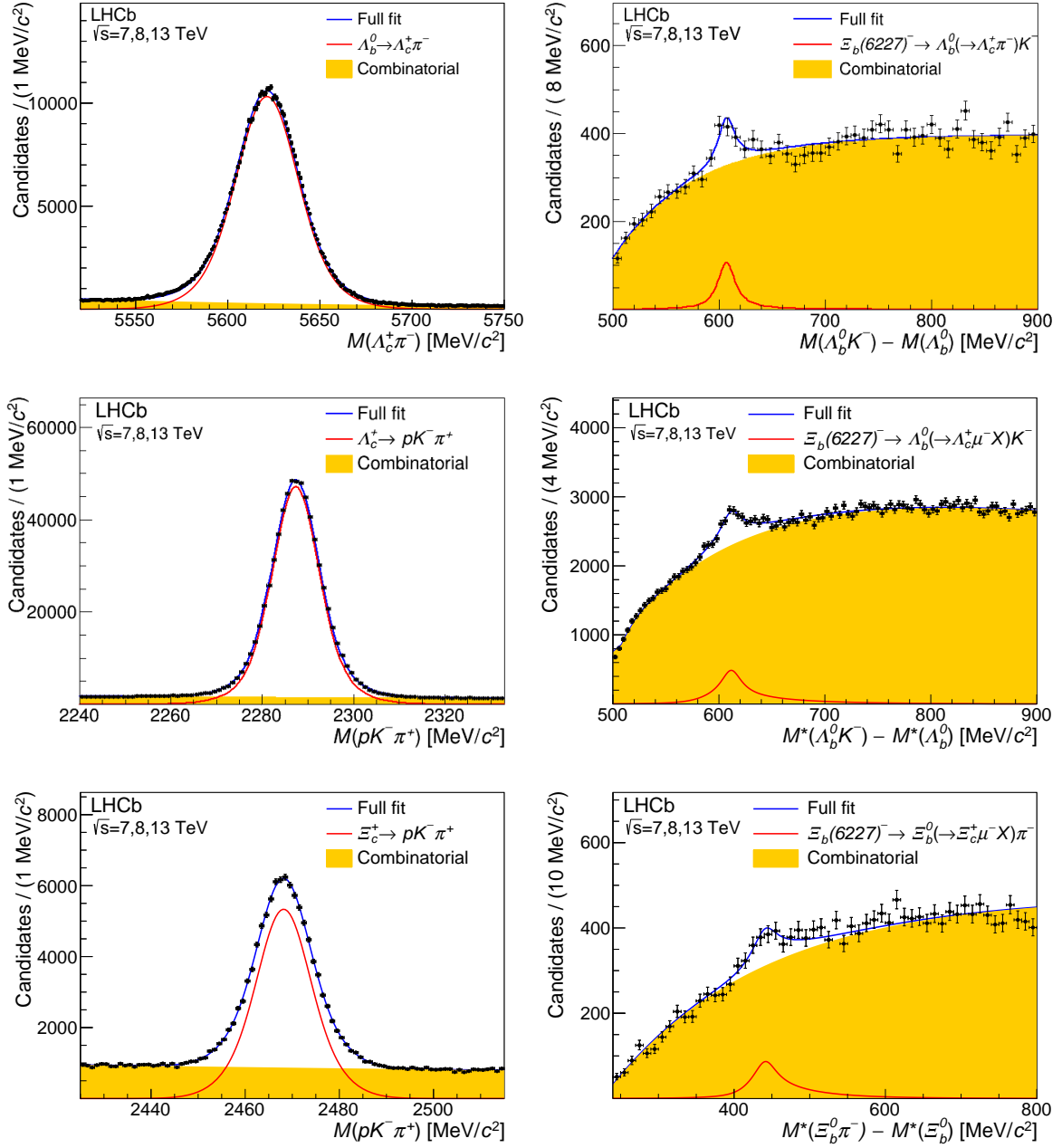


Figure 1: (Left column) Invariant mass spectra for (top row)  $\Lambda_b^0 \rightarrow \Lambda_c^+ \pi^-$ , (middle)  $\Lambda_c^+$  from  $\Lambda_b^0 \rightarrow \Lambda_c^+ \mu^- X$ , and (bottom)  $\Xi_c^+$  from  $\Xi_b^0 \rightarrow \Xi_c^+ \mu^- X$  candidate decays for the combined 7, 8 and 13 TeV data sets. (Right column) Spectra of mass differences for  $\Xi_b(6227)^-$  candidates, reconstructed in the final state shown in the corresponding plot in left column. The symbol  $M^*$  represents the mass after the constraint  $(p_{H_c^+} + p_{\mu^-} + p_{\text{miss}})^2 = m_{H_b^0}^2$  is applied, as described in the text. Fits are overlaid, as described in the text. The  $\Lambda_b^0 \rightarrow \Lambda_c^+ \mu^- X$  mode (top left only) has been prescaled by a factor of ten.